Vibro-acoustic modelling of aircraft structures using Finite Element- informed Statistical Energy Analysis

Abderrazak Mejdi[1]
ESI-North America
12555 High Bluff Drive suite 160, San Diego, CA, 92130, USA

Luca Alimonti[2]
ESI-North America
12555 High Bluff Drive suite 160, San Diego, CA, 92130, USA

Bryce Gardner[3]
ESI-North America
12555 High Bluff Drive suite 160, San Diego, CA, 92130, USA

ABSTRACT

This paper addresses the problem of predicting the structure borne and airborne sound transmission in aircraft using Statistical Energy Analysis (SEA). Often analytical formulations are used to approximate the SEA parameters. In the present prediction method, a finite element (FE)-informed SEA approach is employed. To compute the coupling coefficient, the structure is represented with a repetition of unit cell and an FE model of the unit cell is assigned to evaluate the direct field dynamic stiffness matrix of the SEA subsystems at the connections. An efficient strategy is employed to determine the equivalent material properties of the FE model. Thus, two-dimensional unit cells of different constructions such as composite, sandwich, visco-elastic laminate and ribbed section sections can be used. To evaluate the equivalent properties of multi-layer structures, each layer is assumed as thick laminate with orthotropic orientation. Moreover, rotational inertia and transversal shear, membrane and bending deformations are accounted for. First-order shear deformation theory is employed. The developed approach handles symmetrical layouts of unlimited numbers of transversal compressible or incompressible layers. The accuracy of this modeling approach is confirmed through comparison to alternate validated theoretical approaches. Representative examples of academic and industrial structural response and interior noise predictions for typical load cases are shown and the use of SEA models as a tool for guiding construction of complex structures to meet acoustic performance targets and optimize designs are presented. Conclusions about the application and advantages of this approach are presented.

[1] Abderrazak.mejdi@esi-group.com

[2] Luca.alimonti@ esi-group.com

[3] Bryce.gardner@ esi-group.com

1. INTRODUCTION

Statistical Energy Analysis (SEA) is a technique in which statistical descriptions of a system are employed in order to simplify the analysis of complicated structural-acoustic problems [1]. Detailed analysis of wave motions of complex structural systems such as multi-layer laminate, sandwich or stiffened plates is often difficult to achieve because of the complexity of the structural configuration. Being able to properly characterize complex stiffened or unstiffened multi-layer lightweight structures and derive the modal density and coupling coefficient is essential for SEA analysis. Often, these parameters are determined analytically which might be restricted to limited configurations such as straight-line connection or planar area connection. Recently a more general approach to compute the SEA parameters by means of FE-informed SEA has been developed where an accurate power flow model is defined to model complex configurations [4]. To compute the coupling coefficient, the authors represented the structure with a repetition of unit cell. A three-dimensional (3D) FE model of the unit cell is assigned to evaluate the direct field dynamic stiffness matrix of the SEA subsystems at the connections. However, the usage of 3D unit cell might have some consequences such as the high number of nodes that might lead to an increase of the computational time. Therefore, a homogeneous unit cell with fewer nodes is developed in the present paper. Indeed, many researchers have studied the homogenization of complex structures such as multi-layer panel or stiffened panels with thick composite skin. For instance, Zhou and Crocker [6] analyzed the sound transmission of sandwich panels where the classical sandwich formulation is used to predict the modal density and the coupling loss factor is measured. Other researchers modelled the laminate composite as a two-dimensional problem wherein the displacement field in each lamina is based on Kirchhoff's hypothesis [7-9]. Moreover, most of the existing models neglect the shear and the in-plane contributions as well as the rotational inertia that strongly influence the high-frequency behavior of these structures. More accurate results are provided by a first-order shear deformation theory [10-12] or other higher-order shear deformation theories [13]. The first-order shear deformation theory based on Reissner–Mindlin-type assumptions takes the transverse shear deformation into account. However, it requires shear correction factors to compensate for errors resulting from the approximation of the shear-strain distribution. For instance, the work presented in references [14-15] used Reissner–Mindlin-type assumptions in a Transfer Matrix Method (TMM) context. In reference [16], the authors developed a semi-analytical model to analyze ribbed panels with evenly and unevenly stiffened composite laminate flat structure and the modal density of periodically stiffened beam and plate structures in terms of phase constants, which were associated with propagating wave motion [17]. The distinct behaviour of the stiffened panel in terms of wavenumbers has been described in reference [18]. Recently, a wave and modal based approach are developed to model both sandwich and stiffened or unstiffened panels with thick composite skins in an SEA context [19]. The effect of shear deformation and the in-plane / bending coupling effects are employed to improve the vibro-acoustic response prediction of multi-layer structures. The work presented in [19] is extended in the present paper.

2. THEORY

In what follows a general periodic FE method for modeling wave propagation in SEA subsystems is employed. This approach will be used in a generalized SEA wave-based approach framework.

2.1. Structural response

Consider a two-dimensional structure made of periodic connected elements (or unit cell). The dynamic equilibrium under harmonic motion of the unit cell reads:

$$[\mathbf{K}(\omega) - \omega^2\mathbf{M}(\omega)]\mathbf{q}(\omega) = \mathbf{f}(\omega) \tag{1}$$

where $\mathbf{K}$ and $\mathbf{M}$ are the stiffness and mass matrices, respectively, assumed to be frequency dependent, $\mathbf{q}$ is the nodal Degrees of Freedom (DOFs), $\mathbf{f}$ is the sum of the internal and external forces and ω is the circular frequency. The DOFs of the cell are partitioned as [21]:

$$\mathbf{q} = \{\mathbf{q_I}, \mathbf{q_B}, \mathbf{q_T}, \mathbf{q_L}, \mathbf{q_R}, \mathbf{q_{LB}}, \mathbf{q_{RB}}, \mathbf{q_{LT}}, \mathbf{q_{RT}}, \mathbf{q_I}\}^{\mathbf{T}} \tag{2}$$

where the subscripts refer to internal (I), edges (B, T, L, R) and corner (LB, RB, LT, RT) sets. Moreover, the location of the nodes on opposite edges (*e.g.*, L and R sets) is assumed identical. An equivalent partitioning is used for the vector. A Bloch wave solution is imposed by assuming pseudo-periodic boundary conditions on $\mathbf{q}$ which lead to:

$$[\mathbf{T}_l\ (\mu)[\mathbf{K}(\omega) - \omega^2\mathbf{M}(\omega)]\mathbf{T}\mathrm{r}\ (\mu)]\ \mathbf{q}_0 \ = \ \mathbf{T}_l\ (\mu)\mathbf{f}\mathrm{ext} \quad (3)$$

Where μ is the non-dimensional wavenumber which can be interpreted in the Cartesian coordinate (μ_x, μ_y) and $\mathbf{q}_0 = \{\mathbf{q}_\mathbf{I}, \mathbf{q}_\mathbf{B}, \mathbf{q}_\mathbf{T}, \mathbf{q}_\mathbf{L}, \mathbf{q}_\mathbf{LB}\}^\mathbf{T}$

The wave FE dispersion equation for a given (μ, ω) can be obtained by setting $(\mathrm{f} = 0)$

$$[\mathbf{A}(\omega)]\mathbf{q_0} \ = \ 0 \quad (4)$$

Where **A** is the first term in Eq (3). The solution of the non-linear eigenproblem Eq (4) can be used to construct the dynamic stiffness matrices of each wavefield coupled to each junction. Hence, the components of the SEA power balance equation can be computed [4].

$$\pi\omega[(\boldsymbol{\mathcal{M}}_{\boldsymbol{j}} + \boldsymbol{\mathcal{M}}_{dj} + \textstyle\sum_{k\neq j} h_{k,j})\boldsymbol{C}_j - \sum_{k\neq j} h_{j,k}\boldsymbol{C}_k] = \mathbf{\Pi}_{inj}^{exst}, \quad (5)$$

where $\boldsymbol{\mathcal{M}}_{\boldsymbol{dj}}$ are the damping coefficients, h_{jk} are the coupling terms and $\boldsymbol{C}$ is the diffuse field amplitude.

2.2. Homogenized unit cell

A simple homogeneous 2D unit cell can be used to model complex industrial structures such as composite, sandwich or ribbed panels. The properties of the homogenized unit cell can be determined using the wave dispersion of the structure. This strategy has the advantage of reducing the number of nodes and consequently the number of DOFs required to model complex structures. In the following section a description of the generalized dispersion equation corresponding to different type of structures is presented.

2.2.1 Stiffened structure

The generalized differential equations governing the vibration of the infinite stiffened plate are given by [22]:

$$\frac{\partial N_x}{\partial x} + \frac{\partial N_{xy}}{\partial y} - m_s\frac{\partial^2 U}{\partial t^2} - I_{z2}\frac{\partial^2 \varphi_x}{\partial t^2} = P_{\mathrm{exc}}^{\mathrm{a}} - \sum_{p=-\infty}^{p=+\infty} F_{1,p}^a \ \ y\ \delta\ \ x - pS_x \ - \sum_{q=-\infty}^{q=+\infty} F_{2,q}^t \ \ x\ \delta\ \ y - qS_y \quad (6)$$

$$\frac{\partial N_y}{\partial y} + \frac{\partial N_{yx}}{\partial x} - m_s\frac{\partial^2 V}{\partial t^2} - I_{z2}\frac{\partial^2 \varphi_y}{\partial t^2} = P_{\mathrm{exc}}^{\mathrm{t}} - \sum_{p=-\infty}^{p=+\infty} F_{1,p}^t \ \ y\ \delta\ \ x - pS_x \ - \sum_{q=-\infty}^{q=+\infty} F_{2,q}^a \ \ x\ \delta\ \ y - qS_y \quad (7)$$

$$\frac{\partial Q_x}{\partial x} + \frac{\partial Q_y}{\partial y} - m_s\frac{\partial^2 W}{\partial t^2} = P_{\mathrm{inc}}\big\|_{z=0} + P_{\mathrm{ref}}\big\|_{z=0} - P_{\mathrm{trans}}\big\|_{z=0} - \sum_p F_{1,p}^f \ \ y\ \delta\ \ x - pS_x \ - \sum_q F_{2,q}^f \ \ x\ \delta\ \ y - qS_y \quad (8)$$

$$\frac{\partial M_x}{\partial x} + \frac{\partial M_{xy}}{\partial y} - Q_x - I_z\frac{\partial^2 \varphi_x}{\partial t^2} = -\sum_{p=-\infty}^{p=+\infty} M_{1,p} \ \ y\ \delta\ \ x - qS_x \quad (9)$$

$$\frac{\partial M_y}{\partial y} + \frac{\partial M_{xy}}{\partial x} - Q_y - I_z\frac{\partial^2 \varphi_y}{\partial t^2} = -\sum_{q=-\infty}^{q=+\infty} M_{2,q} \ \ x\ \delta\ \ y - qS_y \quad (10)$$

where N_x, N_y, N_{xy}, M_x, M_y and M_{xy} are the panel in-plane forces and bending moments, Q_x, Q_y, are the panel shearing forces and m_s, I_z and I_{z2} are the total mass per unit area and the rotational inertia terms. Assuming a solution in the form of space-harmonics series truncated to a finite but sufficient number of terms p and q to ensure convergence at the highest frequency of interest:

$$\{e\} = \sum_{pq} \{e_{pq}\} \exp\left(-jk_{x,p}x - jk_{y,q}y\right) \tag{11}$$

Where $j^2 = -1$ and $\{e_{pq}\}$ is the displacement vector. $k_{x,p} = k_{pq}\cos(\gamma_{pq})$ and $k_{y,q} = k_{pq}\sin(\gamma_{pq})$, with k_{pq}, γ_{pq} are the wavenumber module and heading angle for a given $p, q \in \mathbb{N}$. Eq (6-10) can be written in a compact form:

$$[\mathbf{A}_{pq}]\langle e_{pq}\rangle = \langle \mathbf{P}_{exst}\rangle - \langle \mathbf{Q}_{1,0q}\rangle - \langle \mathbf{Q}_{2,p0}\rangle \tag{12}$$

Where $\mathbf{A}_{pq}$ is the skin stiffness matrix and $\mathbf{P}_{exst}$ is the external load vector. $\mathbf{Q}_{1,0q}, \mathbf{Q}_{2,p0}$ are the internal loads applied by the connection on the skin in the *x* and *y* directions. Using the periodicity relation and Poisson's sum formula [22], a set of decoupled equation is found for each space-harmonic p, q:

$$\left[k_{pq}^2[\mathbf{A_2}(\gamma_{\text{pq}})] + jk_{pq}[\mathbf{A_1}(\gamma_{\text{pq}})] + [\mathbf{A_0}(\gamma_{\text{pq}})]\right]\langle e_{pq}\rangle = 0 \tag{13}$$

Where $\mathbf{A}_i\,; i = \{1{:}3\}$ are 5x5 matrices written in terms of a homogenized plate stiffness. Indeed, the skin stiffness is corrected regarding distinct behaviour in terms of wavenumbers of the stiffened panel. The plate behavior shifts from global behaviour, when the half wavelength is bigger than (S_x, S_y), to periodic behaviour over areas delimited by (S_x, L_y) or the area delimited by (L_x, S_y). Finally, when the half-wavelength goes below the rib and frame spacing S_x and S_y, the dynamic behaviour is determined by the behaviour of a uniform subpanel delimited by the ribs and frames (local behaviour). Those four conditions represent the four models required when fully describing the dynamic behaviour of a stiffened plate over a large frequency band [18-19].

2.2.2 Laminate structure dispersion relation

For composite structures, the dynamic equilibrium relations of the unstiffened in-vacuum panel can be obtained by removing the terms of forces and moments in Eq (6-10). Using the constitutive relation between the forces and the displacements [19]. The equations of motion can be obtained by assuming a general solution of the following form:

$$\{e\} = \{U, V, W, \varphi_x, \varphi_y\}^T \exp\left(jk_x + jk_y + j\omega t\right) \tag{14}$$

where $k_x = k_p\cos(\theta)$ and $k_y = k_p\sin(\theta)$ are the components of the structural wave number, k_p is defined as a function of the heading angle θ .This leads to the following compact matrix equation:

$$\{k_p^2[\mathbf{A}_2] + jk_p[\mathbf{A}_1] + [\mathbf{A}_0]\}\{e\} = 0 \tag{15}$$

Where $\mathbf{A}_i$ $\{i = 0{:}3\}$ are 5x5 matrices [19]. The eigenproblem shown in Eq (15) has 10 conjugate eigenvalues corresponding to propagating and evanescent waves.

2.2.3 Sandwich structure

For the sandwich model, a Mindlin-type assumption [10] is used to describe the displacement field of the core. The skins are assumed to be thinner than the core and display bending behavior. Their displacement field is built using the Love-Kirchhoff's assumptions but is corrected to account for the rotational influence of the transversal shearing in the core [14,15,19]. This leads to the following dispersion equation:

$$\{k_p^4[\mathbf{A}_4] + jk_p^3[\mathbf{A}_3] + k_p^2[\mathbf{A}_2] + jk_p[\mathbf{A}_1] + [\mathbf{A}_0]\}\{e\} = 0 \tag{16}$$

Where $\mathbf{A}_i$ $\{i = 0{:}3\}$ are 3x3 matrices. Equation (16) represent a complex polynomial eigenproblem of fourth order which has 12 conjugate eigenvalues corresponding to propagating and evanescent waves.

2. NUMERICAL RESULTS

Various industrial and academic examples are given hereafter and validated by comparison with the VA One commercial software [23]. In the following examples, the wave approach-based predictions using the different homogenized models are examined by comparing various vibro-acoustic indicators with finite element simulations. Both structural and acoustical behavior under structure-borne excitation is investigated. The capabilities and accuracy of the vibration and sound transmission prediction of various types of structures are checked by analyzing their effects.

2.1 Case 1: Non-coplanar coupled subsystems with isolators

In a first example, an SEA system of two coupled rectangular uniform plates is considered (Figure 1-a). The thickness of the two plate-A and plate-B are $1mm$ and $1.5mm$, respectively. The two plates are made of aluminium material and the angle between them is 135 degrees. The area of each plate is 1m^2. A line spring isolator is applied between the line connection and plate-A. The spring stiffness with respect to the coordinate system (x-axis is along the line junction) is $k_x = k_y = k_z = 10$ MPa and $k_{xx} = 0.1$ MPa/rad. The plate-A is excited by a point force. The mean quadratic velocity for the two plates is shown in Figures 1-b-c. The SEA predicted mean quadratic velocity of plate-A and plate-B is found in excellent agreement with the FE reference model. The latter is obtained by averaging 100 velocity sensors randomly located across each plate and solving for 25 different realizations of the nominal system. It is observed that the present approach captures well the physics. Clearly the isolator affects the energy flow through the junction especially at 800Hz where most of the energy is stored in the source plate which lead to a significant deep in the receiver plate structural response.

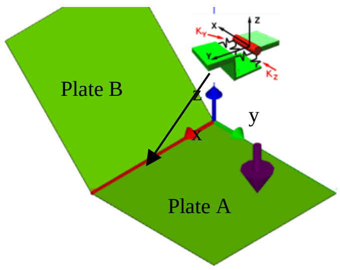

a) Non-coplanar coupled plates.

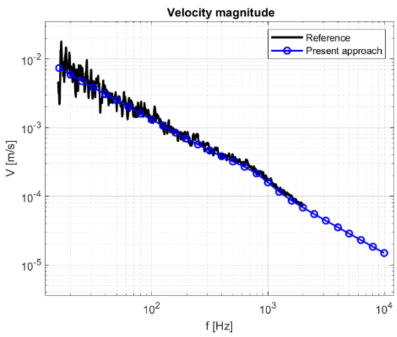

b) Predicted velocity of plate A.

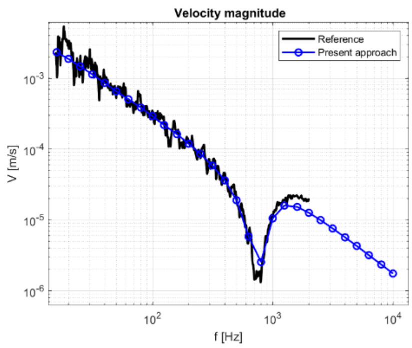

c) Predicted velocity of plate B.

Figure [1]: Comparison of predicted mean quadratic velocity versus finite element prediction for Case 1.

2.2 Case 2: Connected doubly curved shell

In the following example, two coupled composite doubly curved shells are considered (Figure 2-a). The curvature radius of the two plates-A and B are $r1 = 2m$ and $r2 = 7m$, respectively. The two

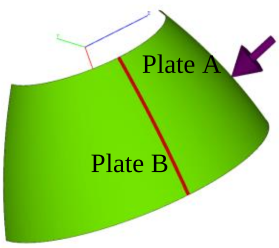

a) coupled doubly curved panels.

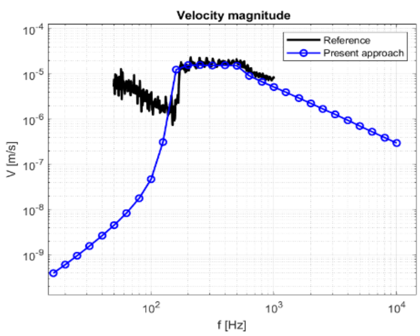

c) Predicted velocity of plate A.

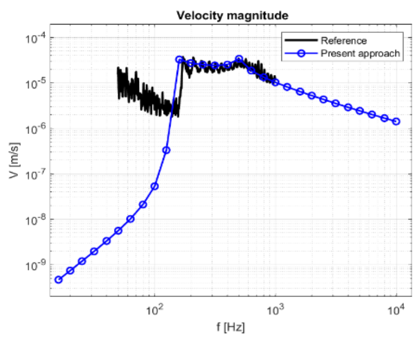

c) Predicted velocity of plate B.

Figure [2]: Comparison of predicted mean quadratic velocity versus finite element prediction in Case 2.

plates are made of 17 layers of orthotropic material. The material orientations of the layup are [45,0,-45,90,90,-45,0,45,0,45,0,-45,90,90,-45,0,45] (in degrees). Again, the predicted mean square velocity is in excellent agreement with the FE solutions shown in Figures 2-c-d. Note that the SEA model assumes large panel subsystems, so below the first mode, the results differ from the FE solution.

2.3 Case 3: Acoustic transmission through curved shell

Next, a curved panel coupled to an acoustic cavity Figure 3-a is investigated. The panel is made of aluminum with thickness of $1mm$. The panel's curvature radius is 2m. The panel is excited by a harmonic point force. The predicted result using the presented approach is compared to FE solution predicted using VA One software [23]. As shown in Figures 3-b-c, the present prediction approach, captures well the physics and corroborate well with the reference FE solution. The pick observed around 700 Hz in both the structural and acoustic response corresponding to the structure's ring frequency. In this example, simply supported boundary conditions on the edge of the plate is considered. It is worth noting that the boundary conductions have an important effect below the coincidence due to the radiation from edges and corners which may explain the small difference in terms of the power input to the acoustic cavity.

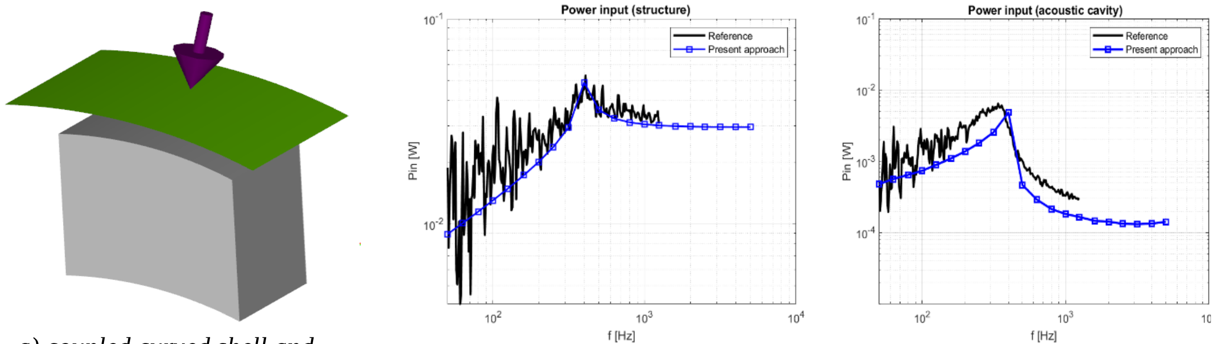

a) coupled curved shell and acoustic cavity. *b) Predcited power input to the structure.* *c) Predcited power input to the acoustic cavity.*

Figure [3]: Comparison of predicted mean quadratic velocity and acoustic response versus finite element prediction in Case 3.

2.4 Case 4: Acoustic transmission through sandwich with light core

In the following example, the accuracy of the presented approach is examined by comparison with the FE solution using VA One [23]. A sandwich with honeycomb core and composite skins coupled to an acoustic cavity is considered (Figure 4-a). The core density is $\rho = 160\ (kg/m^3)$. The Young and shear modulus along *x*-*y*- axis are $Ex = 0.207$GPa, $Ey = 0.322$GPa, $Gxy = 0.09$GPa. The Poisson's ratio $v = 0.15$ and thickness $hs = 6.35mm$.

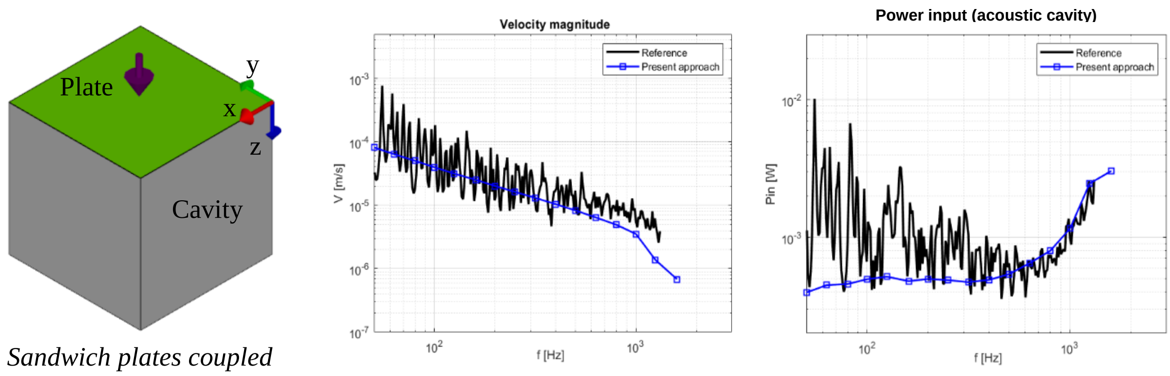

a) Sandwich plates coupled to acoustic cavity. *b) Predicted velocity of the plate.* *c) Predicted power input to the cavity.*

Figure [4]: Comparison of predicted mean quadratic velocity and input power versus finite element prediction for Case 4.

The skins are made of two layers of Graphite/Epoxy with material orientation [45/-45] degrees. Figures 4-b-c, show a comparison between the structure mean square velocity and the power input to the cavity, respectively with FE solution. The predicted result is again in very good agreement with the FE solution.

2.5 Case 5: Structural transmission (aircraft fuselage)

Next, a representative model of an aircraft fuselage made of a curved bidirectionally stiffened panel coupled to a uniform shell Figure 5-a is investigated. The stiffened panel skin is reinforced by orthogonal C and Z shaped ribs as seen in Figure 5-b. The spacing between the C and Z shaped ribs and frame are 0.5m and 0.35m, respectively. The height and thickness of the C-shaped rib are 9.5cm and 2mm, respectively, while the height and thickness of the Z-shaped rib are 2.5cm and 2mm. The two panels are made of aluminum material and the thickness of the two skins is 1mm. The panels' curvature radii are 2m. The uniform panel is excited by a harmonic point force. The predicted power input to the plate-A and mean square velocity of the tow plates are is compared to FE solution. Again, excellent agreement between the present approach and the FE reference is obtained (Figures 5-c-d-e).

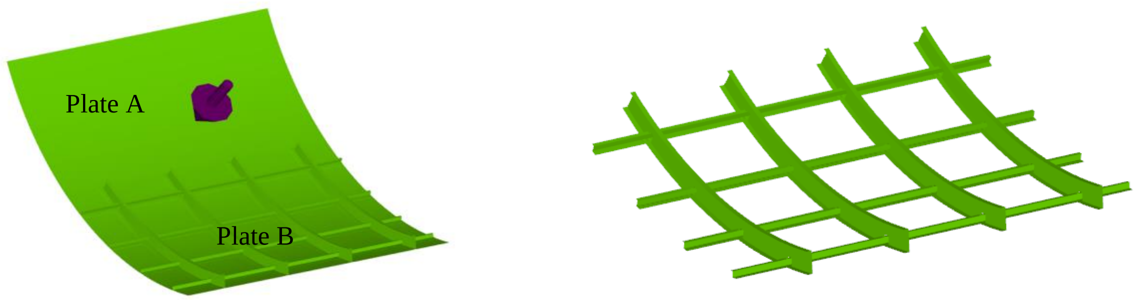

a) coupled panels. *b) Ribs and frame.*

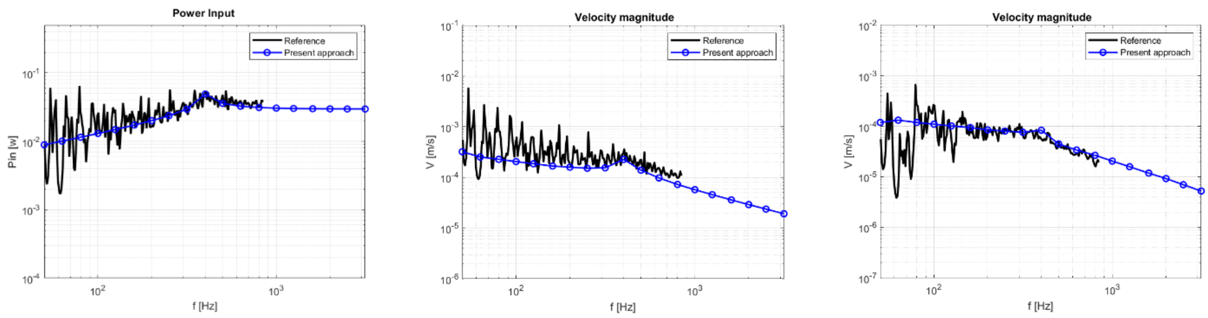

c) Precited power input to plate A. *d) Predicted velocity of plate A.* *e) Predicted velocity of plate B.*

Figure [5]: Comparison of predicted mean quadratic velocity and input power versus finite element prediction in Case 5.

3 CONCLUSIONS

In this paper several academic and industrial configurations are investigated using an FE-informed SEA approach. The problem of predicting the structure-borne and airborne sound transmission is addressed using Statistical Energy Analysis (SEA). To compute the coupling coefficient, the structure is represented with a repetition of unit cell and an FE model of the unit cell is assigned to evaluate the direct field dynamic stiffness matrix of the SEA subsystems at the connections. A homogenized FE model is used to handle complex structures such as composite and stiffened plates. Two-dimensional unit cells of different constructions were enough to accurately evaluate the structural and acoustical response of these structures. To evaluate the equivalent properties of multi-layer structures, each layer is assumed as a thick laminate with orthotropic orientation. Moreover, rotational inertia and transversal shearing, membrane and bending deformations are accounted for. First-order shear deformation theory is employed. The developed approach handles an unlimited number of symmetrical layers of transversal compressible or incompressible layers. The theories are developed in a wave approach context. The structural and acoustical problems are represented within the SEA context and successfully compared to detailed FE predictions.

6. REFERENCES

1. R. Lyon, Statistical energy analysis and structural fuzzy, *Journal of the Acoustical Society of America* 97 (5) (1995) 2878–2881.

2. A. Mejdi and N. Atalla, Dynamic and acoustic response of bidirectionally stiffened panels with eccentric stiffeners subject to airborne and structureborne excitations, *J. Sound. Vib*. 329(21), 4422–4439 (2010).

3. A. Mejdi, J. Legault and Noureddine Atalla, Transmission loss of periodically stiffened laminate composite panels: Shear deformation and in-plane interaction effects. *J. Acoust. Soc. Am*. 131 , 174 (2012)

4. L. Alimonti, N. Atalla, J. Cordioli, The diffuse field reciprocity relationship as a framework for a general power flow model, *NOISE-CON* 2019, San Diego.

5. L. Alimonti, A. Parrinello, SEA model of coupled structures by means of periodic finite element models of the subsystems, *NOISE-CON* 2020.

6. Ran Zhou , Malcolm J. Crocker , Sound transmission loss of foam-filled honeycomb sandwich panels using statistical energy analysis and theoretical and measured dynamic properties. *J. Sound. Vib*. 329 (2010) 673–686.

7. R.S. Langley, The modal density and mode count of the thin cylinders and curved panels, *J. Sound. Vib* 169 (1994).

8. Roussos L. A., Powell C. A., Grosveld F. W. and Koval L. R,. Noise transmission characteristics of advanced composite structural materials, *J. Aircraft*, vol. 21, no.7, 528-535, (1984).

9. J. P. D. Wilkinson, Modal densities of certain shallow structural elements, *J. Acoust. Soc. Am.*, Vol. 43, No. 2, 245-251, 1968.

10. Mindlin RD. Influence of rotatory inertia and shear on flexural motions of isotropic, elastic plates. *ASME J Appl Mech* 1951:1831–8.

11. Nosier A, Kapania RK. Free vibration analysis of laminated plates using a layer-wise theory. In: *AIAA/ASME/ASCE/AHS/ASC structures, structural dynamics, and materials conference no. 34, La Jolla, CA, ETATS-UNIS*, vol. 31 (12); 1993. p. 2335–46.

12. Michael P. Nemeth, A Treatise on Equivalent-Plate Stiffnesses for Stiffened Laminated-Composite Plates and Plate-Like Lattices, *Langley Research Center, Hampton, Virginia, NASA/TP*-2011-216882

13. Reddy, J.N., A simple higher-order theory for laminated composite plates. *ASME J Appl Mech* 1984;51(4):745–52.

14. Ghinet S, and Atalla N., Diffuse field transmission into infinite sandwich composite and laminate composite cylinders. *J Sound Vib* 2006;289(4–5):745–78.

15. Ghinet S, and Atalla N., Vibro-acoustic behaviours of flat sandwich composite panels. *Trans Can Soc Mech Eng* 2006;30(4):473–93.

16. A. Mejdi and N. Atalla, Vibroacoustic analysis of laminated composite panels stiffened by complex laminated composite stiffeners, *International Journal of Mechanical Sciences* 58 (2012) 13–26

17. R.S. Langley, On the modal density and energy flow characteristics of periodic structures, *J. Sound. Vib* 172 (1994) 491–511.

18. P.G. Bremner, Vibro-acoustics of ribbed structures – a compact modal formulation for SEA models, *NOISE-CON* 1994, Ft. Lauderdale, Florida (1994).

19. A. Mejdi, B. Gardner and C. Musser, Vibro-acoustic modeling of sandwich and unribbed or ribbed panels with thick laminate composite skin using Statistical Energy Analysis, DYNCOMP'2015. Arles, France.

20. P. Ramachandran, S. Narayanan, Evaluation of modal density, radiation efficiency and acoustic response of longitudinally stiffened cylindrical shell, *J. Sound. Vib* 304 (2007) 154–174.

21. R.S. Langley. A note on the force boundary conditions for two-dimensional periodic structures with corner freedoms. *J. Sound Vib.* **167**, 377-381,1993

22. A. Mejdi, J. Legault, and N. Atalla, Transmission loss of periodically stiffened laminate composite panels: Shear deformation and in-plane interaction effects, *J. Acoust. Soc. Am.* 131 (1), 2012

23. VA One User's Guide 2021, ESI Group.